DOI: 10.1113/JP277193

# α-MSH increases the activity of MC3R-expressing neurons in the ventral tegmental area

Katherine Stuhrman West[1,2], Chunxia Lu[3], David P. Olson[3], and Aaron G. Roseberry[1,2]

[1]Department of Biology and [2]Neuroscience Institute, Georgia State University, Atlanta, GA

[3]Department of Pediatrics, University of Michigan, Ann Arbor MI

Running title: α-MSH increases the activity of VTA MC3R neurons

Keywords: α-MSH, dopamine, VTA, MC3R

Corresponding Author:

Aaron G. Roseberry

Department of Biology

Georgia State University

PO Box 4010

Atlanta, GA 30302-4010

aroseberry@gsu.edu

Phone: 404-413-5451; Fax: 404-413-5301

**Key Points Summary**

- Alpha-melanocyte stimulating hormone (α-MSH) is an anorexigenic peptide, and injection of the α-MSH analog MTII into the ventral tegmental area (VTA) decreases food and sucrose intake and food reward.
- Melanocortin-3 receptors (MC3R) are highly expressed in the VTA, suggesting that the effects of intra-VTA α-MSH may be mediated by α-MSH changing the activity of MC3R-expressing VTA neurons.
- α-MSH increased the firing rate of MC3R VTA neurons in acute brain slices from mice, but did not affect the firing rate of non-MC3R VTA neurons.
- The α-MSH induced increase in MC3R neuron firing rate is likely activity dependent, and was independent of fast synaptic transmission and intracellular $Ca^{2+}$ levels.
- These results help us to better understand how α-MSH acts in the VTA to affect feeding and other dopamine dependent behaviors.

**Abstract**

The mesocorticolimbic dopamine system, the brain's reward system, regulates multiple behaviors including food intake and food reward. There is substantial evidence that the melanocortin system of the hypothalamus, an important neural circuit controlling feeding and body weight, interacts with the mesocorticolimbic dopamine system to affect feeding, food reward, and body weight. For example, melanocortin-3 receptors (MC3Rs) are expressed in the ventral tegmental area (VTA), and our lab previously showed that intra-VTA injection of the MC3R agonist, MTII, decreases home-cage food intake and operant responding for sucrose pellets. The cellular mechanisms underlying the effects of intra-VTA α-MSH on feeding and food reward are unknown, however. To determine how α-MSH acts in the VTA to affect feeding, we performed electrophysiological recordings in acute brain slices

from mice expressing EYFP in MC3R neurons to test how α-MSH affects the activity of VTA MC3R neurons. α-MSH significantly increased the firing rate of VTA MC3R neurons without altering the activity of non-MC3R expressing VTA neurons. In addition, the α-MSH-induced increase in MC3R neuron activity was independent of fast synaptic transmission and intracellular $Ca^{2+}$ levels. Finally, we show that the effect of α-MSH on MC3R neuron firing rate is likely activity dependent. Overall, these studies provide an important advancement in the understanding of how α-MSH acts in the VTA to affect feeding and food reward.

**Introduction**

The world health organization estimates that obesity rates have nearly tripled worldwide since 1975 (World Health Organization, 2018). The rapid rise in obesity is a major health concern as obesity increases the risk for many diseases such as heart disease, diabetes, cancers, and stroke (Afshin *et al.*, 2017). The increased prevalence of obesity is largely attributed to an increase in food consumption (Finkelstein *et al.*, 2005; Hall *et al.*, 2009; Swinburn *et al.*, 2009; Swinburn *et al.*, 2011). Thus, understanding the mechanisms of food intake and weight gain is important for the development of new effective treatments to prevent and reverse obesity.

The melanocortin system has been widely shown to play an important role in the control of feeding and body weight. This system encompasses two neuronal populations in the arcuate nucleus of the hypothalamus, pro-opiomelanocortin (POMC) expressing neurons and agouti-related protein/neuropeptide-Y (AgRP/NPY) expressing neurons, the peptides released by these neurons, and the downstream receptors of these peptides (Roseberry *et al.*, 2015). POMC is a propeptide that is post-translationally processed to produce the melanocyte stimulating hormones (α-, β-, and γ-MSH). α-, β-, and γ-MSH are agonists to the centrally expressed melanocortin receptors, melanocortin-3 and melanocortin-4 receptors (MC3/4Rs), while AgRP is an inverse-agonist to the MC3/4Rs (Roseberry *et al.*, 2015). AgRP/NPY and POMC neurons respond to an animal's energy state and function in an opposing manner. For example, an energy deficit or hunger state activates AgRP/NPY neurons (Hahn

*et al.*, 1998; Takahashi & Cone, 2005) while an energy surplus or satiated state activates POMC neurons (Singru *et al.*, 2007; Wu *et al.*, 2014). In addition, activation of AgRP/NPY neurons or injection of MC3/4R antagonists increases feeding (Fan *et al.*, 1997; Ollmann *et al.*, 1997; Aponte *et al.*, 2011; Krashes *et al.*, 2011), while activation of POMC neurons or injection of MC3/4R agonists decrease feeding (Fan *et al.*, 1997; Pierroz *et al.*, 2002; Aponte *et al.*, 2011; Zhan *et al.*, 2013). The melanocortin system is clearly an important regulator of food intake, and substantial evidence indicates that this system interacts with other brain nuclei and neural systems, including the mesocorticolimbic dopamine system, to regulate food intake and body weight.

The mesocorticolimbic dopamine system is the primary neural circuit for reward and motivated behavior and also regulates food reward, feeding, and body weight (Wise, 2004; Lutter & Nestler, 2009; Kenny, 2011; Volkow *et al.*, 2011; Roseberry *et al.*, 2015). The mesocorticolimbic dopamine system is comprised of dopamine neurons in the VTA and the downstream targets of dopamine neurons such as the nucleus accumbens (NAc), prefrontal cortex (PFC), olfactory tubercle, and hippocampus. Numerous studies show the importance of dopamine for food intake and food reward. For example, dopamine-deficient mice are aphagic (Zhou & Palmiter, 1995), and blocking dopamine receptors systemically or in the NAc decreases operant responding for food in rats (Beninger *et al.*, 1987; Cousins *et al.*, 1994; Koch *et al.*, 2000). There is also substantial evidence that intra-VTA injection of a number of feeding-related peptides alters food intake and food reward (Liu & Borgland, 2015). This includes injection of analogs of α-MSH and AgRP into the VTA. For example, our lab has shown that injection of the MC3/4R agonist, MTII, directly into the VTA decreases home-cage food intake, the intake of sucrose and saccharin intake in 2-bottle choice tests, and operant responding for sucrose pellets, whereas injection of the MC3/4R antagonist, SHU9119, into the VTA increases home-cage food intake and operant responding for sucrose pellets (Roseberry, 2013; Yen & Roseberry, 2015; Shanmugarajah *et al.*, 2017). Nevertheless, how α-MSH acts in the VTA at the cellular level to regulate feeding and other reward related behaviors is unknown.

Intra-VTA α-MSH may affect food intake and food reward by regulating VTA dopamine neuron activity. This is supported by studies first conducted in the 1980s that showed intra-VTA

injection of α-MSH increases dopamine turnover in the NAc (Torre & Celis, 1986, 1988). Furthermore, intra-VTA α-MSH and MC3/4R agonists increase dopamine dependent behaviors, such as rearing, grooming, and locomotor activity (Torre & Celis, 1986, 1988; Klusa *et al.*, 1999; Sanchez *et al.*, 2001). Additional evidence indicates that the melanocortin and mesocorticolimbic dopamine systems interact. POMC and AgRP neurons project to the VTA (King & Hentges, 2011; Dietrich *et al.*, 2012), and both MC3Rs and MC4Rs are expressed in dopamine and non-dopamine VTA neurons (Roselli-Rehfuss *et al.*, 1993; Liu *et al.*, 2003; Lippert *et al.*, 2014). The MC3R is expressed at much higher levels in the VTA than the MC4R, however (Roselli-Rehfuss *et al.*, 1993; Liu *et al.*, 2003; Lippert *et al.*, 2014), suggesting that the effects of α-MSH and AgRP in the VTA are likely due to actions on MC3Rs. Thus, α-MSH can clearly act in the VTA to affect food intake, food reward, and other reward behaviors, likely through activation of dopamine neurons expressing the MC3R. However, how α-MSH acts on MC3R-expressing VTA dopamine neurons to regulate food intake and reward behavior and to increase dopamine turnover in the NAc is unknown. Thus, in these studies, we tested whether α-MSH alters the activity of VTA MC3R expressing neurons by using electrophysiology in brain slices from transgenic mice expressing EYFP in MC3R neurons.

**Methods**

Ethical Approval: All protocols and procedures were approved by the Institutional Animal Care and Use Committee at Georgia State University (approval reference no. A17016), and conformed to the *NIH Guide for the Care and Use of Laboratory Animals*. The investigators understand and complied with the ethical standards of *The Journal of Physiology* outlined in Grundy 2015 for all experiments (Grundy, 2015).

Animals: Male and female transgenic mice expressing EYFP in MC3R neurons (5-14 weeks old, 20-25 g, fed ad libitum) on a mixed C57/129 background were used in all experiments. Mice were generated by crossing transgenic mice expressing Cre recombinase tethered to the MC3R gene product by a 2A-self-cleaving peptide (Pei *et al.*, 2018) (generously provided by Dr. David P. Olson, University of Michigan) with a Cre inducible EYFP Ai3 transgenic mouse line from The Jackson

laboratory (Stock # 007903). The specificity of Cre expression in MC3R neurons was previously confirmed in a separate article describing the creation and validation of this mouse (Pei *et al.*, 2018). A total of 84 neurons from 60 mice were used in the experiments described below. Five neurons from 4 mice were excluded from the study because the identity of the neuron was unconfirmed or the neuron died during the experiment.

RNAscope In Situ Hybridization (ISH) assay: RNAscope ISH was performed as previously described (Pei *et al.*, 2018). Briefly, adult mice were quickly decapitated under anesthesia. The brains were then removed, flash frozen with 2-methylbutane at -20ºC, and stored at -80ºC. Coronal brain sections (16 μm) were cut with a cryostat and thaw mounted onto Super Frost Plus Slides (Fisher). ISH was performed according to the RNAscope® 2.5 HD Duplex Detection Kit User Manual for Fresh Frozen Tissue (Advanced Cell Diagnostics, Inc.). The following probes were used: RNAscope® Probe-Mm-Mc3r-C1, Cat No. 412541; RNAscope® Probe-Cre-C2, Cat No. 312281-C2.

Slice preparation and Electrophysiology: Acute brain slices were prepared similar to what has been previously described (Roseberry *et al.*, 2007; Stuhrman & Roseberry, 2015; West & Roseberry, 2017). Briefly, adult mice were anesthetized with isofluorane and decapitated. The brain was then removed and placed in carbogen (95% $O_2$ and 5% $CO_2$) saturated ice-cold sucrose cutting solution containing (in mM) 205 sucrose, 2.5 KCl, 0.5 $CaCl_2$, 1.25 $NaH_2PO_4$, 7.5 $MgCl_2$, 11.1 glucose, 21.4 $NaHCO_3$, and 0.6 kynurenic acid. A brain block containing the VTA was made, and pseudo-horizontal sections (220 μm) were cut with a vibrating blade microtome. Slices were then incubated in artificial cerebral spinal fluid (aCSF) containing (in mM) 126 NaCl, 2.5 KCl, 2.4 $CaCl_2$, 1.2 $NaH_2PO_4$, 1.2 $MgCl_2$, 11.1 glucose, 21.4 $NaHCO_3$, and 1 kynurenic acid at ~ 35°C for ~ 30 min and then transferred to aCSF lacking kynurenic acid for storage before recording. Slices were placed in a recording chamber and perfused with carbogen-saturated aCSF at a flow rate of approximately 1-2 ml/min. Whole-cell and loose cell-attached recordings were made using an Axon multiclamp 700B microelectrode amplifier and Axograph software. MC3R-expressing neurons were identified by the presence of EYFP using a fluorescence microscope and were patch-clamped under gradient contrast optics.

Cell firing was recorded in either the loose-cell attached or whole-cell configuration. Loose cell-attached recordings were obtained with electrodes (7.0-10.0 MΩ) filled with a Na-HEPES based internal solution containing (in mM) 135 Na-HEPES and 20 NaCl, adjusted to 290 mOsm with water. Whole-cell recordings were obtained with electrodes (2.0-3.0 MΩ) filled with a potassium gluconate (KGluconate) based internal solution containing (in mM) 128 KGluconate, 10 NaCl, 1 $MgCl_2$, 10 HEPES, 2 ATP, 0.3 GTP, 10 creatine phosphate, 10 BAPTA or 1 EGTA, and 0.1% biocytin. The internal solution contained EGTA for the experiments examining the effect of α-MSH on MC3R neuron activity under reduced calcium buffering conditions. The internal solution contained BAPTA for all other whole-cell recordings. Corrections were not made for the liquid junction potential, which was calculated to be the following for each internal solution used: KGluconate 10 mM BAPTA, 13.9; KGluconate 1 mM EGTA, 14.7. Series resistance values were approximately 3-15 MΩ. If the series resistance increased by more than 20%, the experiment was terminated or excluded from analysis. The basic action potential characteristics of VTA MC3R and non-MC3R neurons were analyzed using the event detection protocol in Axograph. Briefly, spontaneously firing action potentials (e.g. spontaneous firing in the absence of current injection) were captured using the event detection protocol, which aligns all action potentials at threshold. The rise time (10-90%) and action potential half-width (at 50% max amplitude) were then obtained from the values calculated by Axograph and the average values were calculated for each individual cell. To measure hyperpolarization-activated cation currents (H-current), neurons were voltage clamped at -60 mV and 2 s voltage steps were applied in increasing increments of -10 mV from -50 to -100 mV with a 1 s inter-step interval. Cell firing was recorded in voltage-clamp mode for loose-cell attached recordings and current-clamp mode for whole-cell recordings. Whole-cell recordings were conducted in the presence of fast synaptic blockers (10 μM DNQX and 100 μM picrotoxin), and if the cell was not firing positive current was injected (5- 55 pA). In addition, if the cell stopped firing or did not fire for at least 1 min during baseline recordings or during the first 2 min of adding α-MSH, the experiment was terminated or excluded from analysis. Membrane potential was recorded in current-clamp mode in the presence of tetrodotoxin (1 μM, TTX). For experiments testing the effect of α-MSH on membrane current,

neurons were voltage-clamped at -60 mV, and slow voltage ramps were applied from -100 mV to 0 mV at 100 mV $s^{-1}$ every 30 s in the presence of TTX. For experiments testing the effect of α-MSH on current-step evoked action potentials, the neurons were held at ~ -70 mV and 2 s current steps of 5 pA were applied at increasing amplitudes (5-50 pA) with a 1 s inter-step interval. The current-step protocol was repeated every minute, and if the current steps failed to evoke action potentials or if the number of evoked action potentials decreased over time during baseline recording, the experiment was terminated. The effects of α-MSH on all parameters (change in firing rate, membrane potential, current, or membrane resistance) were determined by averaging the baseline value for the entire 5 minutes prior to the addition of α-MSH, and comparing that to the average value of the 4-6 minute period after the addition of α-MSH. These time points were analyzed for all cells regardless of any apparent differences in the timing of the α-MSH effect between cells. For all experiments, cells were held for at least 10 min prior to drug application to allow for diffusion of the internal solution into the cell and to ensure stability of the recording prior to drug addition.

Immunohistochemistry: To identify VTA neurons used in electrophysiology experiments as dopamine or non-dopamine neurons, 0.1% biocytin was included in the internal pipette solution, and the slices were fixed and stained for tyrosine hydroxylase (TH) post-hoc. After the recording was terminated, the pipette was slowly removed from the neuron to allow the membrane to reseal. The brain slices were transferred to 4% paraformaldehyde and incubated at 4°C for 1-4 days, followed by washing and storage in phosphate-buffered saline (PBS) at 4°C until processing. Brain slices were then incubated with blocking buffer (5% normal goat serum, 0.2% triton X-100, and 0.1% bovine serum albumin (BSA) in PBS) for 6 hours at room temperature. The brain slices were then washed with PBS and incubated with a mouse monoclonal anti-TH antibody (1:1500, Millipore Cat# MAB318, Lot# NG1752067; RRID:AB_2201528) in antibody incubation buffer (0.2% triton X-100, and 1% BSA in PBS) overnight at 4˚C. Brain slices were washed with PBS the next day and incubated with streptavidin Alexa Fluor 594 (1:1000, Invitrogen) and goat anti-mouse Alexa Fluor 647 (1:300, Jackson ImmunoResearch) in antibody incubation buffer for 4 hours at room temperature. The brain slices were then mounted to slides with gelvatol mounting media containing 10% DABCO

and imaged at 20X with a confocal microscope (Carl Zeiss LSM 700). Recorded neurons were identified as either TH-positive, TH-negative, or unidentifiable. Recorded neurons positive for biocytin (red fluorescence) and TH (magenta fluorescence) were identified as TH-positive, and neurons positive for biocytin but negative for TH were identified as TH-negative (Fig. 2I). Recorded neurons were labeled as unidentifiable if the brain slice containing the recorded neuron was damaged during processing, if a biocytin labeled neuron could not be located in the brain slice, or if multiple neurons were labeled for biocytin (which precluded the identification of the exact cell used in the experiment).

Drugs: α-MSH was purchased from Bachem (Torrance, CA). TTX was purchased from Tocris Biosciences (Minneapolis, MN). All other reagents were from common commercial sources.

Data Analysis and Statistics: Data are represented as the mean +/- SEM unless otherwise noted. Data were stored and analyzed using Axograph X (v1.3.5), LabChart (v7.3.6; ADInstruments), and Excel (v14.0; Microsoft Corporation) software. Statistics were calculated using SigmaStat (v11.0; Systat Software, Inc.). To test the hypothesis that α-MSH changes the activity of VTA MC3R and non-MC3R neurons (firing rate, membrane potential, membrane resistance, rheobase, etc.), data were initially tested for normality using the Shapiro-Wilk test and were then analyzed with Student's paired t-tests, under the assumption of normality, or with Wilcoxon signed-rank tests as appropriate. To test the hypothesis that the electrical properties and action potentials of MC3R and non-MC3R VTA neurons are different, data were initially tested for normality using the Shapiro-Wilk test and were then analyzed with Student's t-tests, under the assumption of normality, or with Mann-Whitney U test as appropriate. To test the hypothesis that α-MSH increases the number of current-step evoked action potentials we used a two-way repeated measures ANOVA with Tukey's post-hoc tests, under the assumption of normality. A significance level of $p<0.05$ was set *a priori*. In general, approximately 5-8 cells from 5-7 mice were used in experiments examining the effects of α-MSH on VTA neuron activity.

**Results**

We identified MC3R-expressing VTA neurons ('VTA MC3R neurons') for electrophysiological recordings by visualizing EYFP in cells from transgenic mice that specifically express EYFP in MC3R-expressing neurons. These mice were generated by crossing mice expressing Cre recombinase in MC3R neurons (*MC3R*$^{Cre}$) (Pei *et al.*, 2018) with a Cre inducible EYFP mouse line (Fig. 1A). MC3R neurons were located in the medial VTA spanning the entire anterior-posterior extent of the VTA (Fig. 1A-B). The specificity of Cre expression in MC3R-expressing neurons of *MC3R*$^{Cre}$ mice was previously confirmed in the arcuate nucleus, ventromedial nucleus, and the lateral hypothalamus (Pei *et al.*, 2018). We extended this study and also tested the specificity of Cre expression in the VTA using RNAscope ISH in *MC3R*$^{Cre}$ mice. MC3R and Cre mRNAs were also colocalized in the VTA, demonstrating that Cre is specifically expressed in MC3R-expressing neurons within the VTA of *MC3R*$^{Cre}$ mice (Fig. 1C-E).

We first characterized the electrical properties of VTA MC3R neurons, as VTA MC3R neurons are a novel population of VTA neurons that have not been previously described. We measured capacitance, membrane resistance, and the presence of H-current in 59 MC3R neurons and 12 neighboring non-MC3R neurons. VTA MC3R neurons had a significantly smaller capacitance (Fig. 2A; MC3R neuron, 13.27 +/- 0.50 pF; Non-MC3R neuron, 23.06 +/- 1.32 pF; Mean difference = 9.79; $p<0.001$; Mann-Whitney U test) and a significantly greater membrane resistance than non-MC3R neurons (Fig. 2B; MC3R neuron, 2.12 +/- 0.16 GΩ; Non-MC3R neuron, 0.79 +/- 0.16 GΩ; Mean difference = 1.33; $p<0.001$; Mann-Whitney U test). H-current was present in 34 out of 59 of the MC3R neurons tested and was present in all 12 non-MC3R neurons tested (Fig. 2C-D). H-current was significantly smaller when the cell was stepped from -60 mV to -100 mV in MC3R neurons compared to non-MC3R neurons, however (Fig. 2E; MC3R neuron, -13.08 +/- 2.22 pA; Non-MC3R neuron, -62.28 +/- 19.96 pA; Mean difference = 49.2; $p<0.001$; Mann-Whitney U test). We also examined the basic action potential characteristics of spontaneously firing MC3R and non-MC3R neurons measured with whole-cell current clamp. The average action potential height of MC3R neurons and non-MC3R neurons were 63.66 +/- 2.6 mV and 64.9 mV +/- 2.54 mV, respectively, with

no significant difference between the two groups (Mean difference = 1.24; p=0.748; Student's t test). The action potential half-width and rise time of MC3R neurons were significantly greater than the action potential half-width and rise time of non-MC3R neurons, however (Fig. 2F-H, Half-width: MC3R neuron, 2.76 +/- 0.33 ms; Non-MC3R neuron, 1.54 +/- 0.23 ms; Mean difference = 1.22; p=0.014; Student's t test (F); Rise time: MC3R neuron, 1.01 +/- 0.15 ms; Non-MC3R neuron, 0.62 +/- 0.07 ms; Mean difference = 0.39; p=0.019; Mann Whitney U test (G)). We filled a portion of the recorded MC3R and non-MC3R neurons with biocytin and then performed post-recording immunohistochemistry for TH to identify the recorded neurons as dopamine or non-dopamine neurons. Twelve of the 38 VTA MC3R neurons filled with biocytin were reliably identified as TH-positive and 7 of the 38 as TH-negative (Fig. 2A-B, E, I). Three of the 8 non-MC3R neurons filled with biocytin were reliably identified as TH-positive, while none were identified as TH-negative (Fig. 1A-B, E, I). For both the MC3R and non-MC3R neurons, the remaining cells either could not be conclusively identified or were damaged during processing. Thus, MC3Rs are expressed in both dopamine and non-dopamine VTA neurons, and VTA MC3R neurons are smaller than non-MC3R neurons, have a higher membrane resistance, little to no H-current, and broader action potentials.

To determine whether α-MSH affects the activity of VTA MC3R neurons, we first tested whether α-MSH changed the spontaneous firing rate of VTA MC3R neurons in the loose-cell attached configuration. α-MSH (1 μM) significantly increased the spontaneous firing rate of VTA MC3R neurons by 0.41 +/- 0.07 Hz (Fig. 3; before α-MSH, 2.92 +/- 0.41 Hz; after α-MSH, 3.33 +/- 0.39 Hz; p<0.001; Student's paired t test). Out of the 8 MC3R neurons tested, all exhibited an action potential width ≥1.2 ms suggesting that the MC3R neurons tested were dopaminergic. A broad action potential width is a physiological characteristic that is indicative of dopamine neurons and has repeatedly and reliably been used to identify dopamine neurons in cell-attached and extracellular recordings (Ungless *et al.*, 2004; Ford *et al.*, 2006; Chieng *et al.*, 2011). However, we could not use post-recording immunohistochemistry to identify dopamine neurons in these experiments, and without validation cannot conclusively classify these neurons as dopaminergic. Thus, α-MSH increases the firing of VTA putative dopamine neurons expressing MC3Rs.

We next confirmed and extended these findings by testing whether α-MSH increases the firing rate of VTA MC3R neurons in the whole-cell current-clamp configuration. We included blockers of fast synaptic currents (10 μM DNQX, 100 μM picrotoxin) in the bath solution to confirm that the α-MSH induced increase in MC3R neuron firing rate was due to direct action on MC3Rs and not changes in synaptic transmission. α-MSH (1 μM) significantly increased the firing rate of MC3R neurons by 0.42 +/- 0.11 Hz in the presence of fast synaptic blockers (Fig. 4A-C; before α-MSH, 1.17 +/- 0.21 Hz; after α-MSH, 1.59 +/- 0.15 Hz; p=0.012; Student's paired t test). Intracellular $Ca^{2+}$ plays a key role in VTA dopamine neuron excitability, firing rate, and burst firing (Grace & Bunney, 1984b, a; Paladini & Roeper, 2014), so we next tested whether reduced $Ca^{2+}$ buffering affected the α-MSH induced increase in MC3R neuron firing rate using an internal solution containing a low $Ca^{2+}$ buffer (1 mM EGTA). α-MSH (1 μM) also significantly increased the firing rate of MC3R neurons using the 1 mM EGTA internal solution by 0.51 +/- 0.17 Hz (Fig. 4D-E; before α-MSH, 1.28 +/- 0.34 Hz; after α-MSH, 1.78 +/- 0.47 Hz; p=0.028; Student's paired t test), with no significant difference between the magnitudes of α-MSH induced increase in firing rate between the two groups (10 mM BAPTA, 0.42 +/- 0.11 Hz vs. 1 mM EGTA, 0.51 +/- 0.17 Hz; Mean difference = 0.09; p=0.673; Student's t test). Thus, α-MSH increases the firing rate of VTA MC3R neurons through a mechanism independent of fast synaptic transmission and intracellular $Ca^{2+}$ levels. To identify whether these MC3R neurons were dopaminergic, we labeled the MC3R neurons with biocytin and stained for TH. Five out of 12 were TH-positive, and we were unable to reliably identify the remaining 7 neurons. These experiments further confirm that α-MSH increases the firing rate of VTA dopamine neurons expressing MC3Rs.

MC3Rs are only expressed in a subset of VTA neurons (Lippert *et al.*, 2014), and there is some low level expression of MC4Rs in the VTA (Roselli-Rehfuss *et al.*, 1993; Liu *et al.*, 2003; Lippert *et al.*, 2014), so we next tested whether the α-MSH induced increase in VTA MC3R neuron firing rate was specific to VTA MC3R neurons. In these experiments we tested the effect of α-MSH on non-MC3R neuron activity under the exact same conditions used to test the effect of α-MSH on MC3R neuron activity (e.g. in whole-cell current-clamp configuration with blockers of fast synaptic

currents; Fig. 4C). α-MSH did not increase the firing rate of non-MC3R expressing VTA neurons (Fig. 5; before α-MSH, 0.70 +/- 0.14 Hz, after α-MSH: 0.49 +/- 0.13 Hz; p=0.104; Student's paired t test). There was a trend toward a decrease in firing rate (-0.2 +/- 0.11 Hz), but this decrease was not statistically significant (Fig. 5C). The non-MC3R neurons tested were stained for TH, and 3 out of 5 neurons tested were TH-positive, while 2 could not reliably be identified. Therefore, α-MSH does not increase the firing rate of non-MC3R expressing dopamine neurons, and the α-MSH induced increase in VTA neuron firing appears to be specific to VTA MC3R neurons.

α-MSH could increase the activity of VTA MC3R neurons by direct depolarization or by modifying the firing properties of the cell (e.g. threshold) independent of a direct change in membrane potential. To determine if α-MSH directly depolarizes MC3R neurons, we tested the effect of α-MSH on membrane potential in the presence of TTX (1 μM), DNQX (10 μM), and picrotoxin (100 μM). α-MSH (1 μM) slightly increased the membrane potential of MC3R neurons, but this increase was not statistically significant (Fig. 6A-B; before α-MSH, -53.7 +/- 3.7 mV; after α-MSH -52.4 +/- 3.6 mV; Mean depolarization = 1.34 +/- 0.84 mV; p=0.177; Student's paired t test). To confirm and extend our results, we used voltage clamp to test the effect of α-MSH on membrane current and slow voltage ramps (-100 mV to 0 mV 100 mV $s^{-1}$) in the presence of TTX (1 μM), DNQX (10 μM), and picrotoxin (100 μM). α-MSH (1 μM) did not affect membrane current or membrane resistance in VTA MC3R neurons (Fig. 6C-D; $R_M$ before α-MSH, 1,413.61 +/- 292.72 MΩ; $R_M$ after α-MSH 1,276.18 +/- 210.7 MΩ; Mean difference = 137.43; p=0.156; Wilcoxin signed-rank test). The MC3R neurons tested in these experiments were also stained for TH, and 4 out of 12 were TH-positive, 3 were TH-negative, and 5 could not be reliably identified.

We then tested whether α-MSH altered VTA MC3R neuron firing independent of a direct depolarization by testing the effect of α-MSH on current-step evoked action potentials. The neurons were held at ~ -70 mV and a set of current steps of increasing amplitude (5-50 pA in 5 pA increments; 2 s each; 1 s inter-step interval) were applied every minute. α-MSH (1 μM) did not significantly affect rheobase (the minimal current required to reach threshold potential and generate an action potential) (Fig. 7B,E; before α-MSH, 26.9 +/- 3.5 pA; after α-MSH, 25 +/- 3 pA; Mean difference =

1.9; p=0.351; Student's paired t test) or membrane potential (Fig. 7C-D; before α-MSH, -70.6 +/- 0.87 mV; after α-MSH, -68.1 +/- 1.7 mV; Mean difference = 2.5; p=0.181; Student's paired t test). However, α-MSH (1 μM) did significantly increase the number of current-evoked action potentials at the 35, 40, 45, and 50 pA current steps in MC3R neurons (Fig. 7A-B; significant main effect of current step ($F(9, 63)=22.135$, $p<0.001$) and significant current-step× α-MSH interaction ($F(9,63)=3.227$, $p=0.003$; two-way repeated measures ANOVA). The current-step evoked action potentials were further analyzed at the 40 pA current step, because this step consistently evoked 3-4 action potentials at baseline in 7 out of 8 neurons tested. One cell was excluded from this analysis, because the 40 pA current step failed to consistently evoke action potentials. α-MSH significantly decreased the inter-spike interval at the 40 pA current step (Fig. 7F; before α-MSH, 119.7 +/- 20.8 ms; after α-MSH, 90.9 +/- 12.1 ms; Mean difference = 28.8; p=0.016; Wilcoxin signed-rank test), and there was a trend towards a decrease in the latency to the first spike at the 40 pA current step (Fig. 7G; before α-MSH, 1.07 +/- 0.13 sec; after α-MSH, 0.85 +/- 0.07 sec; Mean difference = 0.22; p=0.131; Student's paired t test). Thus, α-MSH facilitates MC3R neuron firing through an activity dependent mechanism that does not appear to involve direct depolarization or a change in rheobase or threshold potential. Consistent with our other experiments, we stained these MC3R neurons for TH, and 1 out of 8 were identified as TH-positive, 4 as TH-negative, and 3 could not be reliably identified. Thus, these results suggest α-MSH increases the firing rate of both dopamine and non-dopamine VTA MC3R neurons.

**Discussion**

In these studies we have shown that α-MSH significantly increases the firing rate of VTA MC3R neurons through an activity dependent mechanism, as α-MSH increased the activity of MC3R neurons only when the neurons were firing. α-MSH did slightly increase the membrane potential of MC3R neurons; therefore, it is possible that this slight increase in membrane potential caused a significant increase in MC3R neuron firing. In addition, α-MSH did not affect rheobase in MC3R neurons, suggesting that α-MSH does not increase the firing rate of MC3R neurons by lowering threshold potential. Furthermore, α-MSH increased the firing rate through a mechanism independent

of fast synaptic transmission and intracellular $Ca^{2+}$ levels. Thus, our results suggest α-MSH increases the firing rate of VTA MC3R neurons through an activity dependent mechanism that is independent of intracellular $Ca^{2+}$ levels or altered synaptic transmission onto VTA MC3R neurons.

The VTA is comprised of a heterogeneous population of neurons including dopamine, GABA, and glutamate neurons that have different projection targets, electrophysiological characteristics, and molecular markers (Morales & Margolis, 2017). We examined the electrophysiological characteristics of VTA MC3R neurons and found that they had a significantly smaller capacitance compared to non-MC3R neurons suggesting that MC3R neurons are smaller than non-MC3R neurons. In addition, VTA MC3R neurons had a significantly higher membrane resistance, little to no H-current, and a greater action potential half-width and rise time compared to non-MC3R neurons. Previous studies have shown that the highest levels of VTA MC3R neurons are found in the ventromedial region of the VTA (Lippert *et al.*, 2014), and for our experiments, recorded VTA MC3R neurons were located in more medial regions of the VTA, while recorded non-MC3R neurons were located in the central to more lateral regions of the VTA. Our results and the location of MC3R neurons suggests that VTA dopamine neurons expressing MC3Rs likely project to the medial PFC (mPFC), NAc core, NAc medial shell, or basolateral amygdala, as VTA dopamine neurons projecting to these areas are significantly smaller than dopamine neurons projecting to the NAc lateral shell and are primarily located in the medial posterior VTA (Lammel *et al.*, 2008). Furthermore, it was previously shown that VTA dopamine neurons projecting to the basolateral amygdala and NAc medial shell have a significantly smaller capacitance, higher membrane resistance, and little to no H-current compared to NAc lateral shell projecting dopamine neurons (Baimel *et al.*, 2017). In addition, mPFC, NAc core, NAc medial shell, and basolateral amygdala projecting VTA dopamine neurons have wider action potentials compared to the action potentials of NAc lateral shell projecting dopamine neurons (Lammel *et al.*, 2008; Baimel *et al.*, 2017). Thus, the electrical properties of VTA MC3R neurons suggest that dopamine neurons expressing MC3Rs most likely project to the mPFC, NAc core, NAc medial shell, or basolateral amygdala and do not project to the NAc lateral shell, but further experiments are needed to determine the projection targets of VTA MC3R neurons.

MC3Rs are expressed in both VTA dopamine and non-dopamine neurons (dopamine: ~ 57%; non-dopamine: ~43%) (Lippert *et al.*, 2014). The identity of MC3R non-dopamine neurons is currently unknown, and these neurons may be GABAergic or glutamatergic neurons, as both are found in the VTA (Yamaguchi *et al.*, 2007; Nair-Roberts *et al.*, 2008; Margolis *et al.*, 2012). Previous studies have shown that intra-VTA α-MSH increases dopamine release in the NAc and dopamine-dependent behaviors suggesting that α-MSH increases VTA dopamine neuron activity (Torre & Celis, 1986, 1988; Klusa *et al.*, 1999; Lindblom *et al.*, 2001; Sanchez *et al.*, 2001; Jansone *et al.*, 2004). In addition, γ-MSH increased the firing rate of a subset of VTA dopamine neurons in rats (Pandit *et al.*, 2016). In agreement, our results suggest that α-MSH increases the firing rate of VTA dopamine neurons expressing MC3Rs. All of the MC3R neurons tested in the cell-attached recordings had broad action potential widths (≥ 1.2 ms), which has been shown to reliably identify mouse VTA dopamine neurons in cell-attached recordings (Ford *et al.*, 2006; Chieng *et al.*, 2011), suggesting that the neurons recorded in our cell-attached experiments are putative dopamine neurons. In addition, 12 of the MC3R neurons tested in our experiments were TH positive. Nevertheless, our results also suggest that α-MSH increases the firing rate of VTA non-dopamine MC3R neurons, as 7 MC3R neurons were TH negative. Thus, α-MSH likely increases the firing rate of dopamine and non-dopamine VTA MC3R neurons. In conclusion, we have shown that α-MSH increases the firing rate of VTA dopamine MC3R-expressing neurons, but α-MSH may increase the firing rate of VTA GABA and/or glutamate MC3R-expressing neurons as well, and further studies will be required to conclusively identify the specific subtypes of VTA MC3R neurons responding to α-MSH.

Altering VTA dopamine neuron activity and downstream dopamine release affects food intake and feeding behavior, but how VTA dopamine neuron activity regulates feeding behavior is complex and not completely understood (Palmiter, 2007; Kenny, 2011; Volkow *et al.*, 2011). For example, increasing dopamine neuron activity and dopamine release can both increase and decrease food intake. Indeed, increasing dopamine release in the NAc using a low dose of amphetamine increases food intake while higher doses decrease food intake in rats (Evans & Vaccarino, 1986), and anorexigenic (feeding inhibiting) and orexigenic (feeding stimulating) peptides have both been shown

to increase dopamine neuron activity while having opposite effects on food intake (Liu & Borgland, 2015). Furthermore, different anorexigenic peptides decrease food intake by either increasing or decreasing dopamine neuron activity and dopamine release depending on the peptide (Liu & Borgland, 2015). For example, the anorexigenic peptides insulin and leptin decrease dopamine neuron activity and feeding (Hommel *et al.*, 2006; Labouebe *et al.*, 2013; Thompson & Borgland, 2013), but α-MSH increases NAc dopamine release (Torre & Celis, 1986, 1988; Lindblom *et al.*, 2001; Sanchez *et al.*, 2001; Jansone *et al.*, 2004) and decreases feeding (Roseberry, 2013; Yen & Roseberry, 2015; Shanmugarajah *et al.*, 2017). How α-MSH increased NAc dopamine release at the cellular level to regulate feeding behavior was previously unknown, however. Here we have identified a novel mechanism for the control of VTA MC3R neuron activity by α-MSH. As a result, these studies provide a better understanding of how α-MSH acts in the VTA at the cellular level and suggest intra-VTA α-MSH decreases food intake and food reward by increasing the activity of a specific population of VTA dopamine and non-dopamine neurons through an activity dependent mechanism.

The effect of α-MSH on VTA MC3R neurons likely occurs through activation of MC3Rs, as MC3Rs are highly expressed in the VTA (Roselli-Rehfuss *et al.*, 1993; Lippert *et al.*, 2014). It is possible that α-MSH could mediate its effect on MC3R neurons by acting on MC4Rs as well, but this seems unlikely. Although MC4Rs are also expressed in the VTA, they are expressed at much lower levels compared to MC3Rs (Roselli-Rehfuss *et al.*, 1993; Liu *et al.*, 2003; Lippert *et al.*, 2014), and MC4Rs are most abundantly expressed in caudal regions of the VTA, while MC3Rs are expressed throughout the rostral-caudal extent of the VTA (Lippert *et al.*, 2014). Thus, although we cannot rule out the possibility that the effects of α-MSH on VTA MC3R neuron activity are also mediated by MC4Rs in some of the MC3R neurons tested, this does not seem likely.

We also showed that α-MSH does not significantly increase the firing rate of non-MC3R expressing VTA neurons, but there was a trend toward a decrease in firing rate in these studies, as α-MSH reduced the firing rate of 4 out of 5 of the non-MC3R neurons tested. This decrease in firing rate may be due to run down, because the firing rate slowly ran down in most of the recorded neurons.

Alternatively, α-MSH may decrease the firing rate of non-MC3R expressing VTA dopamine neurons through activation of dopamine D2 receptors (D2R). VTA dopamine neurons release dopamine from their soma and dendrites (Bjorklund & Lindvall, 1975; Geffen *et al.*, 1976; Kalivas & Duffy, 1991; Rice *et al.*, 1997; Beckstead *et al.*, 2004), and this somatodendritic release inhibits neighboring dopamine neurons through D2R mediated activation of G-coupled inward rectifying potassium (GIRK) channels (Aghajanian & Bunney, 1977; Lacey *et al.*, 1987; Mercuri *et al.*, 1997; Beckstead *et al.*, 2004). Our results suggest α-MSH increases the firing rate of VTA dopamine-MC3R neurons, so the increased activity of dopamine-MC3R neurons could have caused an increase in somatodendritic dopamine release and inhibition of neighboring VTA dopamine neurons, but this possibility remains to be tested.

The exact mechanisms by which α-MSH increases VTA MC3R neuron activity is unknown. MC3Rs are G protein-coupled receptors that signal through $G_s$ and thus activate adenylyl cyclase and subsequently cAMP and protein kinase A (PKA) (Roselli-Rehfuss *et al.*, 1993). However, additional experiments have demonstrated that the MC3R is coupled to other G-proteins and can activate other signaling pathways. For example, activating MC3Rs in HEK293 cells also activates MAP kinase through a Gi protein-PI3K signaling pathway (Chai *et al.*, 2007). Thus, it is possible that α-MSH increases VTA MC3R neuron activity by activating PKA, MAPK, or PI3K and subsequently increasing or decreasing the conductance of an ion channel current through its phosphorylation. Indeed, reducing M-current (a voltage-gated potassium current) in VTA dopamine neurons significantly decreases the inter-spike interval of evoked action potentials (Koyama & Appel, 2006), and blocking A-type current (a low-threshold voltage-gated potassium current) increases the firing rate and the inward inter-spike current in VTA dopamine neurons (Khaliq & Bean, 2008). Thus, α-MSH could increase the firing rate of VTA MC3R neurons by reducing M-current or A-type current as α-MSH did significantly decrease the inter-spike interval of evoked action potentials in VTA MC3R neurons. In addition, α-MSH could increase the firing rate of MC3R neurons by increasing the conductance of a $Na^+$ current as spontaneous firing in VTA dopamine neurons is primarily dependent on two $Na^+$ currents, a tetrodotoxin (TTX) insensitive $Na^+$ leak current, and a TTX-sensitive voltage-

dependent $Na^+$ current (Khaliq & Bean, 2010; Gantz *et al.*, 2018). Finally, it is also possible that α-MSH directly increases VTA MC3R neuron activity simply through a direct depolarization, as α-MSH did slightly depolarize MC3R neurons, but this change in membrane potential was not statistically significant making it difficult to determine the contribution of this change to the observed increase in firing. Thus, further experiments are needed to determine how α-MSH increases VTA MC3R neuron firing rate, and to identify the intracellular signaling pathway mediating these effects.

In summary, we have shown that α-MSH increases the firing rate of MC3R expressing VTA neurons through an activity dependent mechanism. These results advance our understanding of the cellular mechanisms through which intra-VTA α-MSH regulates food intake, food reward, and other dopamine dependent behaviors, and how intra-VTA α-MSH increases dopamine turnover in the NAc.

**References**

Afshin A, Forouzanfar MH, Reitsma MB, Sur P, Estep K, Lee A, Marczak L, Mokdad AH, Moradi-Lakeh M, Naghavi M, Salama JS, Vos T, Abate KH, Abbafati C, Ahmed MB, Al-Aly Z, Alkerwi A, Al-Raddadi R, Amare AT, Amberbir A, Amegah AK, Amini E, Amrock SM, Anjana RM, Arnlov J, Asayesh H, Banerjee A, Barac A, Baye E, Bennett DA, Beyene AS, Biadgilign S, Biryukov S, Bjertness E, Boneya DJ, Campos-Nonato I, Carrero JJ, Cecilio P, Cercy K, Ciobanu LG, Cornaby L, Damtew SA, Dandona L, Dandona R, Dharmaratne SD, Duncan BB, Eshrati B, Esteghamati A, Feigin VL, Fernandes JC, Furst T, Gebrehiwot TT, Gold A, Gona PN, Goto A, Habtewold TD, Hadush KT, Hafezi-Nejad N, Hay SI, Horino M, Islami F, Kamal R, Kasaeian A, Katikireddi SV, Kengne AP, Kesavachandran CN, Khader YS, Khang YH, Khubchandani J, Kim D, Kim YJ, Kinfu Y, Kosen S, Ku T, Defo BK, Kumar GA, Larson HJ, Leinsalu M, Liang X, Lim SS, Liu P, Lopez AD, Lozano R, Majeed A, Malekzadeh R, Malta DC, Mazidi M, McAlinden C, McGarvey ST, Mengistu DT, Mensah GA, Mensink GBM, Mezgebe HB, Mirrakhimov EM, Mueller UO, Noubiap JJ, Obermeyer CM, Ogbo FA, Owolabi MO, Patton GC, Pourmalek F, Qorbani M, Rafay A, Rai RK, Ranabhat CL, Reinig N, Safiri S, Salomon JA, Sanabria JR, Santos IS, Sartorius B, Sawhney M, Schmidhuber J, Schutte AE, Schmidt MI, Sepanlou SG, Shamsizadeh M, Sheikhbahaei S, Shin MJ, Shiri R, Shiue I, Roba HS, Silva DAS, Silverberg JI, Singh JA, Stranges S, Swaminathan S, Tabares-Seisdedos R, Tadese F, Tedla BA, Tegegne BS, Terkawi AS, Thakur JS, Tonelli M, Topor-Madry R, Tyrovolas S, Ukwaja KN, Uthman OA, Vaezghasemi M, Vasankari T, Vlassov VV, Vollset SE, Weiderpass E, Werdecker A, Wesana J, Westerman R, Yano Y, Yonemoto N, Yonga G, Zaidi Z, Zenebe ZM, Zipkin B & Murray CJL. (2017). Health Effects of Overweight and Obesity in 195 Countries over 25 Years. *N Engl J Med* **377,** 13-27.

Aghajanian GK & Bunney BS. (1977). Dopamine"autoreceptors": pharmacological characterization by microiontophoretic single cell recording studies. *Naunyn Schmiedebergs Arch Pharmacol* **297,** 1-7.

Aponte Y, Atasoy D & Sternson SM. (2011). AGRP neurons are sufficient to orchestrate feeding behavior rapidly and without training. *Nat Neurosci* **14,** 351-355.

Baimel C, Lau BK, Qiao M & Borgland SL. (2017). Projection-Target-Defined Effects of Orexin and Dynorphin on VTA Dopamine Neurons. *Cell Rep* **18,** 1346-1355.

Beckstead MJ, Grandy DK, Wickman K & Williams JT. (2004). Vesicular dopamine release elicits an inhibitory postsynaptic current in midbrain dopamine neurons. *Neuron* **42,** 939-946.

Beninger RJ, Cheng M, Hahn BL, Hoffman DC, Mazurski EJ, Morency MA, Ramm P & Stewart RJ. (1987). Effects of extinction, pimozide, SCH 23390, and metoclopramide on food-rewarded operant responding of rats. *Psychopharmacology (Berl)* **92,** 343-349.

Bjorklund A & Lindvall O. (1975). Dopamine in dendrites of substantia nigra neurons: suggestions for a role in dendritic terminals. *Brain Res* **83,** 531-537.

Chai B, Li JY, Zhang W, Ammori JB & Mulholland MW. (2007). Melanocortin-3 receptor activates MAP kinase via PI3 kinase. *Regul Pept* **139,** 115-121.

Chieng B, Azriel Y, Mohammadi S & Christie MJ. (2011). Distinct cellular properties of identified dopaminergic and GABAergic neurons in the mouse ventral tegmental area. *J Physiol* **589,** 3775-3787.

Cousins MS, Wei W & Salamone JD. (1994). Pharmacological characterization of performance on a concurrent lever pressing/feeding choice procedure: effects of dopamine antagonist, cholinomimetic, sedative and stimulant drugs. *Psychopharmacology (Berl)* **116,** 529-537.

Dietrich MO, Bober J, Ferreira JG, Tellez LA, Mineur YS, Souza DO, Gao XB, Picciotto MR, Araujo I, Liu ZW & Horvath TL. (2012). AgRP neurons regulate development of dopamine neuronal plasticity and nonfood-associated behaviors. *Nat Neurosci* **15,** 1108-1110.

Evans KR & Vaccarino FJ. (1986). Intra-nucleus accumbens amphetamine: dose-dependent effects on food intake. *Pharmacol Biochem Behav* **25,** 1149-1151.

Fan W, Boston BA, Kesterson RA, Hruby VJ & Cone RD. (1997). Role of melanocortinergic neurons in feeding and the agouti obesity syndrome. *Nature* **385,** 165-168.

Finkelstein EA, Ruhm CJ & Kosa KM. (2005). Economic causes and consequences of obesity. *Annu Rev Public Health* **26,** 239-257.

Ford CP, Mark GP & Williams JT. (2006). Properties and opioid inhibition of mesolimbic dopamine neurons vary according to target location. *J Neurosci* **26,** 2788-2797.

Gantz SC, Ford CP, Morikawa H & Williams JT. (2018). The Evolving Understanding of Dopamine Neurons in the Substantia Nigra and Ventral Tegmental Area. *Annu Rev Physiol* **80,** 219-241.

Geffen LB, Jessell TM, Cuello AC & Iversen LL. (1976). Release of dopamine from dendrites in rat substantia nigra. *Nature* **260,** 258-260.

Grace AA & Bunney BS. (1984a). The control of firing pattern in nigral dopamine neurons: burst firing. *J Neurosci* **4,** 2877-2890.

Grace AA & Bunney BS. (1984b). The control of firing pattern in nigral dopamine neurons: single spike firing. *J Neurosci* **4,** 2866-2876.

Grundy D. (2015). Principles and standards for reporting animal experiments in The Journal of Physiology and Experimental Physiology. *J Physiol* **593,** 2547-2549.

Hahn TM, Breininger JF, Baskin DG & Schwartz MW. (1998). Coexpression of Agrp and NPY in fasting-activated hypothalamic neurons. *Nat Neurosci* **1,** 271-272.

Hall KD, Guo J, Dore M & Chow CC. (2009). The progressive increase of food waste in America and its environmental impact. *PLoS One* **4,** e7940.

Hommel JD, Trinko R, Sears RM, Georgescu D, Liu ZW, Gao XB, Thurmon JJ, Marinelli M & DiLeone RJ. (2006). Leptin receptor signaling in midbrain dopamine neurons regulates feeding. *Neuron* **51,** 801-810.

Jansone B, Bergstrom L, Svirskis S, Lindblom J, Klusa V & Wikberg JE. (2004). Opposite effects of gamma(1)- and gamma(2)-melanocyte stimulating hormone on regulation of the dopaminergic mesolimbic system in rats. *Neurosci Lett* **361,** 68-71.

Kalivas PW & Duffy P. (1991). A comparison of axonal and somatodendritic dopamine release using in vivo dialysis. *J Neurochem* **56,** 961-967.

Kenny PJ. (2011). Reward mechanisms in obesity: new insights and future directions. *Neuron* **69,** 664-679.

Khaliq ZM & Bean BP. (2008). Dynamic, nonlinear feedback regulation of slow pacemaking by A-type potassium current in ventral tegmental area neurons. *J Neurosci* **28,** 10905-10917.

Khaliq ZM & Bean BP. (2010). Pacemaking in dopaminergic ventral tegmental area neurons: depolarizing drive from background and voltage-dependent sodium conductances. *J Neurosci* **30,** 7401-7413.

King CM & Hentges ST. (2011). Relative number and distribution of murine hypothalamic proopiomelanocortin neurons innervating distinct target sites. *PLoS One* **6,** e25864.

Klusa V, Svirskis S, Opmane B, Muceniece R & Wikberg JE. (1999). Behavioural responses of gamma-MSH peptides administered into the rat ventral tegmental area. *Acta Physiol Scand* **167,** 99-104.

Koch M, Schmid A & Schnitzler HU. (2000). Role of muscles accumbens dopamine D1 and D2 receptors in instrumental and Pavlovian paradigms of conditioned reward. *Psychopharmacology (Berl)* **152,** 67-73.

Koyama S & Appel SB. (2006). Characterization of M-current in ventral tegmental area dopamine neurons. *J Neurophysiol* **96,** 535-543.

Krashes MJ, Koda S, Ye C, Rogan SC, Adams AC, Cusher DS, Maratos-Flier E, Roth BL & Lowell BB. (2011). Rapid, reversible activation of AgRP neurons drives feeding behavior in mice. *J Clin Invest* **121,** 1424-1428.

Labouebe G, Liu S, Dias C, Zou H, Wong JC, Karunakaran S, Clee SM, Phillips AG, Boutrel B & Borgland SL. (2013). Insulin induces long-term depression of ventral tegmental area dopamine neurons via endocannabinoids. *Nat Neurosci* **16,** 300-308.

Lacey MG, Mercuri NB & North RA. (1987). Dopamine acts on D2 receptors to increase potassium conductance in neurones of the rat substantia nigra zona compacta. *J Physiol* **392,** 397-416.

Lammel S, Hetzel A, Hackel O, Jones I, Liss B & Roeper J. (2008). Unique properties of mesoprefrontal neurons within a dual mesocorticolimbic dopamine system. *Neuron* **57,** 760-773.

Lindblom J, Opmane B, Mutulis F, Mutule I, Petrovska R, Klusa V, Bergstrom L & Wikberg JE. (2001). The MC4 receptor mediates alpha-MSH induced release of nucleus accumbens dopamine. *Neuroreport* **12,** 2155-2158.

Lippert RN, Ellacott KL & Cone RD. (2014). Gender-specific roles for the melanocortin-3 receptor in the regulation of the mesolimbic dopamine system in mice. *Endocrinology* **155,** 1718-1727.

Liu H, Kishi T, Roseberry AG, Cai X, Lee CE, Montez JM, Friedman JM & Elmquist JK. (2003). Transgenic mice expressing green fluorescent protein under the control of the melanocortin-4 receptor promoter. *J Neurosci* **23,** 7143-7154.

Liu S & Borgland SL. (2015). Regulation of the mesolimbic dopamine circuit by feeding peptides. *Neuroscience* **289,** 19-42.

Lutter M & Nestler EJ. (2009). Homeostatic and hedonic signals interact in the regulation of food intake. *J Nutr* **139,** 629-632.

Margolis EB, Toy B, Himmels P, Morales M & Fields HL. (2012). Identification of rat ventral tegmental area GABAergic neurons. *PLoS One* **7,** e42365.

Mercuri NB, Saiardi A, Bonci A, Picetti R, Calabresi P, Bernardi G & Borrelli E. (1997). Loss of autoreceptor function in dopaminergic neurons from dopamine D2 receptor deficient mice. *Neuroscience* **79,** 323-327.

Morales M & Margolis EB. (2017). Ventral tegmental area: cellular heterogeneity, connectivity and behaviour. *Nat Rev Neurosci* **18,** 73-85.

Nair-Roberts RG, Chatelain-Badie SD, Benson E, White-Cooper H, Bolam JP & Ungless MA. (2008). Stereological estimates of dopaminergic, GABAergic and glutamatergic neurons in the ventral tegmental area, substantia nigra and retrorubral field in the rat. *Neuroscience* **152,** 1024-1031.

Ollmann MM, Wilson BD, Yang YK, Kerns JA, Chen Y, Gantz I & Barsh GS. (1997). Antagonism of central melanocortin receptors in vitro and in vivo by agouti-related protein. *Science* **278,** 135-138.

Paladini CA & Roeper J. (2014). Generating bursts (and pauses) in the dopamine midbrain neurons. *Neuroscience* **282C,** 109-121.

Palmiter RD. (2007). Is dopamine a physiologically relevant mediator of feeding behavior? *Trends Neurosci* **30,** 375-381.

Pandit R, Omrani A, Luijendijk MC, de Vrind VA, Van Rozen AJ, Ophuis RJ, Garner K, Kallo I, Ghanem A, Liposits Z, Conzelmann KK, Vanderschuren LJ, la Fleur SE & Adan RA. (2016). Melanocortin 3 Receptor Signaling in Midbrain Dopamine Neurons Increases the Motivation for Food Reward. *Neuropsychopharmacology* **41,** 2241-2251.

Pei H, Patterson CM, Sutton AK, Burnett KH, Myers MG, Jr. & Olson DP. (2018). Lateral hypothalamic Mc3R-expressing neurons modulate locomotor activity, energy expenditure and adiposity in male mice. *Endocrinology*.

Pierroz DD, Ziotopoulou M, Ungsunan L, Moschos S, Flier JS & Mantzoros CS. (2002). Effects of acute and chronic administration of the melanocortin agonist MTII in mice with diet-induced obesity. *Diabetes* **51,** 1337-1345.

Rice ME, Cragg SJ & Greenfield SA. (1997). Characteristics of electrically evoked somatodendritic dopamine release in substantia nigra and ventral tegmental area in vitro. *J Neurophysiol* **77,** 853-862.

Roseberry AG. (2013). Altered feeding and body weight following melanocortin administration to the ventral tegmental area in adult rats. *Psychopharmacology (Berl)* **226,** 25-34.

Roseberry AG, Painter T, Mark GP & Williams JT. (2007). Decreased vesicular somatodendritic dopamine stores in leptin-deficient mice. *J Neurosci* **27,** 7021-7027.

Roseberry AG, Stuhrman K & Dunigan AI. (2015). Regulation of the mesocorticolimbic and mesostriatal dopamine systems by alpha-melanocyte stimulating hormone and agouti-related protein. *Neurosci Biobehav Rev* **56,** 15-25.

Roselli-Rehfuss L, Mountjoy KG, Robbins LS, Mortrud MT, Low MJ, Tatro JB, Entwistle ML, Simerly RB & Cone RD. (1993). Identification of a receptor for gamma melanotropin and other

proopiomelanocortin peptides in the hypothalamus and limbic system. *Proc Natl Acad Sci U S A* **90,** 8856-8860.

Sanchez MS, Barontini M, Armando I & Celis ME. (2001). Correlation of increased grooming behavior and motor activity with alterations in nigrostriatal and mesolimbic catecholamines after alpha-melanotropin and neuropeptide glutamine-isoleucine injection in the rat ventral tegmental area. *Cell Mol Neurobiol* **21,** 523-533.

Shanmugarajah L, Dunigan AI, Frantz KJ & Roseberry AG. (2017). Altered sucrose self-administration following injection of melanocortin receptor agonists and antagonists into the ventral tegmental area. *Psychopharmacology (Berl)* **234,** 1683-1692.

Singru PS, Sanchez E, Fekete C & Lechan RM. (2007). Importance of melanocortin signaling in refeeding-induced neuronal activation and satiety. *Endocrinology* **148,** 638-646.

Stuhrman K & Roseberry AG. (2015). Neurotensin inhibits both dopamine- and GABA-mediated inhibition of ventral tegmental area dopamine neurons. *J Neurophysiol* **114,** 1734-1745.

Swinburn B, Sacks G & Ravussin E. (2009). Increased food energy supply is more than sufficient to explain the US epidemic of obesity. *Am J Clin Nutr* **90,** 1453-1456.

Swinburn BA, Sacks G, Hall KD, McPherson K, Finegood DT, Moodie ML & Gortmaker SL. (2011). The global obesity pandemic: shaped by global drivers and local environments. *Lancet* **378,** 804-814.

Takahashi KA & Cone RD. (2005). Fasting induces a large, leptin-dependent increase in the intrinsic action potential frequency of orexigenic arcuate nucleus neuropeptide Y/Agouti-related protein neurons. *Endocrinology* **146,** 1043-1047.

Thompson JL & Borgland SL. (2013). Presynaptic leptin action suppresses excitatory synaptic transmission onto ventral tegmental area dopamine neurons. *Biol Psychiatry* **73,** 860-868.

Torre E & Celis ME. (1986). Alpha-MSH injected into the substantia nigra or intraventricularly alters behavior and the striatal dopaminergic activity. *Neurochem Int* **9,** 85-89.

Torre E & Celis ME. (1988). Cholinergic mediation in the ventral tegmental area of alpha-melanotropin induced excessive grooming: changes of the dopamine activity in the nucleus accumbens and caudate putamen. *Life Sci* **42,** 1651-1657.

Ungless MA, Magill PJ & Bolam JP. (2004). Uniform inhibition of dopamine neurons in the ventral tegmental area by aversive stimuli. *Science* **303,** 2040-2042.

Volkow ND, Wang GJ & Baler RD. (2011). Reward, dopamine and the control of food intake: implications for obesity. *Trends Cogn Sci* **15,** 37-46.

West KS & Roseberry AG. (2017). Neuropeptide-Y alters VTA dopamine neuron activity through both pre- and postsynaptic mechanisms. *J Neurophysiol* **118,** 625-633.

Wise RA. (2004). Dopamine, learning and motivation. *Nat Rev Neurosci* **5,** 483-494.

World Health Organization (2017, October 18). Obesity and Overweight. Retrieved from http://www.who.int/en/news-room/fact-sheets/detail/obesity-and-overweight.

Wu Q, Lemus MB, Stark R, Bayliss JA, Reichenbach A, Lockie SH & Andrews ZB. (2014). The temporal pattern of cfos activation in hypothalamic, cortical, and brainstem nuclei in response to fasting and refeeding in male mice. *Endocrinology* **155,** 840-853.

Yamaguchi T, Sheen W & Morales M. (2007). Glutamatergic neurons are present in the rat ventral tegmental area. *Eur J Neurosci* **25,** 106-118.

Yen HH & Roseberry AG. (2015). Decreased consumption of rewarding sucrose solutions after injection of melanocortins into the ventral tegmental area of rats. *Psychopharmacology (Berl)* **232,** 285-294.

Zhan C, Zhou J, Feng Q, Zhang JE, Lin S, Bao J, Wu P & Luo M. (2013). Acute and long-term suppression of feeding behavior by POMC neurons in the brainstem and hypothalamus, respectively. *J Neurosci* **33,** 3624-3632.

Zhou QY & Palmiter RD. (1995). Dopamine-deficient mice are severely hypoactive, adipsic, and aphagic. *Cell* **83,** 1197-1209.



**Additional Information**

Competing interests: The authors do not have any competing interests.

Author Contributions: The experiments were conducted in the laboratory of Aaron G Roseberry at Georgia State University. KSW conducted the experiments and drafted the manuscript. DPO generated and provided the MC3R-Cre mice, and CL and DPO performed the RNAscope ISH experiments. KSW and AGR analyzed and interpreted the results of the experiments. KSW and AGR conceived and designed the work. KSW wrote the initial draft of the manuscript, and KSW, AGR, and DPO revised the manuscript.

Funding: Funds for these studies were provided by The Brains and Behavior Program at Georgia State University and NIH grant 1R01DK115503 (to AGR).

**Figure Legends**

Fig. 1: Expression of EYFP in MC3R neurons of the VTA from a *MC3R*$^{Cre}$-EYFP mouse, and localization of Cre and MC3R transcripts in the VTA from a *MC3R*$^{Cre}$ mouse. A-B. Expression of EYFP in coronal brain slices containing the VTA from a *MC3R*$^{Cre}$-EYFP mouse that expresses EYFP in MC3R neurons. (anterior VTA—bregma -3.28 (A), middle/posterior VTA—bregma -3.4 (B)). C-E. Colocalization of MC3R mRNA (blue) and Cre mRNA (red) in coronal brain slices containing the VTA from a *MC3R*$^{Cre}$ mouse using RNAscope ISH at 4x (C), 20x (D), and 40x (E). Scale bars: 500 μm (A-C), 100 μm (D); 50 μm (E).

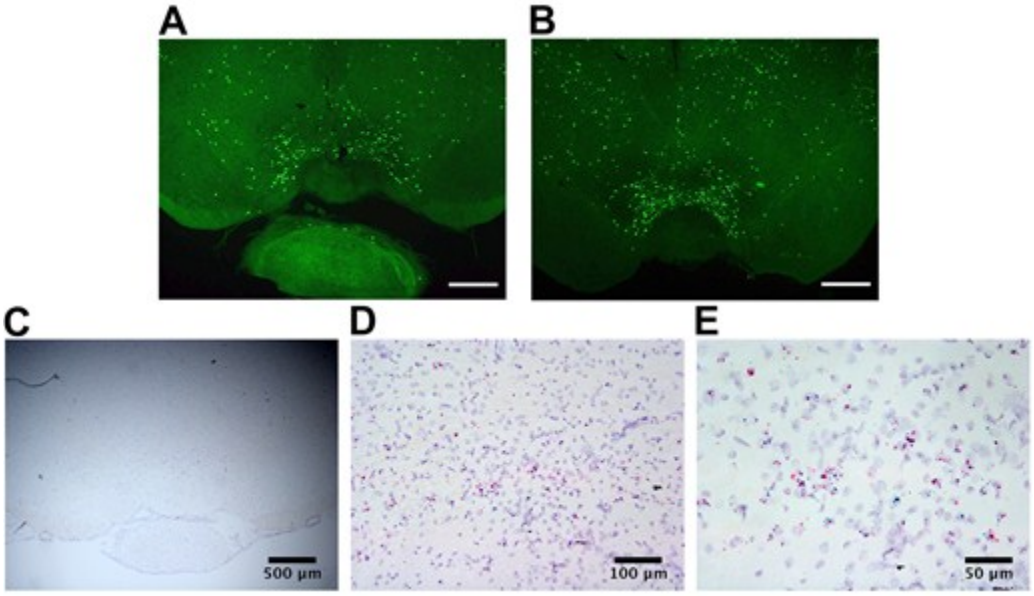

Fig. 2: Characteristics of VTA MC3R neurons. A-B. Average capacitance (A) and membrane resistance ($R_M$, B) of VTA MC3R and non-MC3R neurons. C. Sample traces from MC3R neurons without (dark-grey trace) or with (black trace) H-current, and a sample trace of H-current in a non-MC3R neuron (light-grey trace). D. Average amplitude of H-current at -60, -70, -80, -90, and -100 mV for MC3R neurons without H-current, MC3R neurons with H-current, and non-MC3R neurons. E. Average amplitude of H-current at -100 mV for MC3R neurons with H-current and non-MC3R neurons. F-G. Average action potential (AP) half-width (F) and rise time (G) of spontaneously firing VTA MC3R and non-MC3R neurons. H. Sample traces of an action potential from a VTA MC3R and a non-MC3R neuron. I. Example of a TH+ (a.-c.) and a TH- (d.-f.) recorded VTA neuron. Neurons were filled with biocytin and labeled for biocytin (red, a. and d.) and TH (magenta, b. and e). Colocalization of TH and biocytin (c. and f.). MC3R neurons: n= 59 cells from 45 mice. Non-MC3R neurons: n= 12 cells from 8 mice. MC3R neurons, H-current: n= 34 cells from 30 mice. MC3R neurons, no H-current: n= 25 cells from 24 mice. F-G: MC3R neurons: n= 12 cells from 9 mice, Non-MC3R neurons: n= 8 cells from 6 mice. Scale bars: C, 30 pA/500 ms. H, 20 mV/5 ms. ** $p<0.001$ *$p<0.05$

Fig. 2

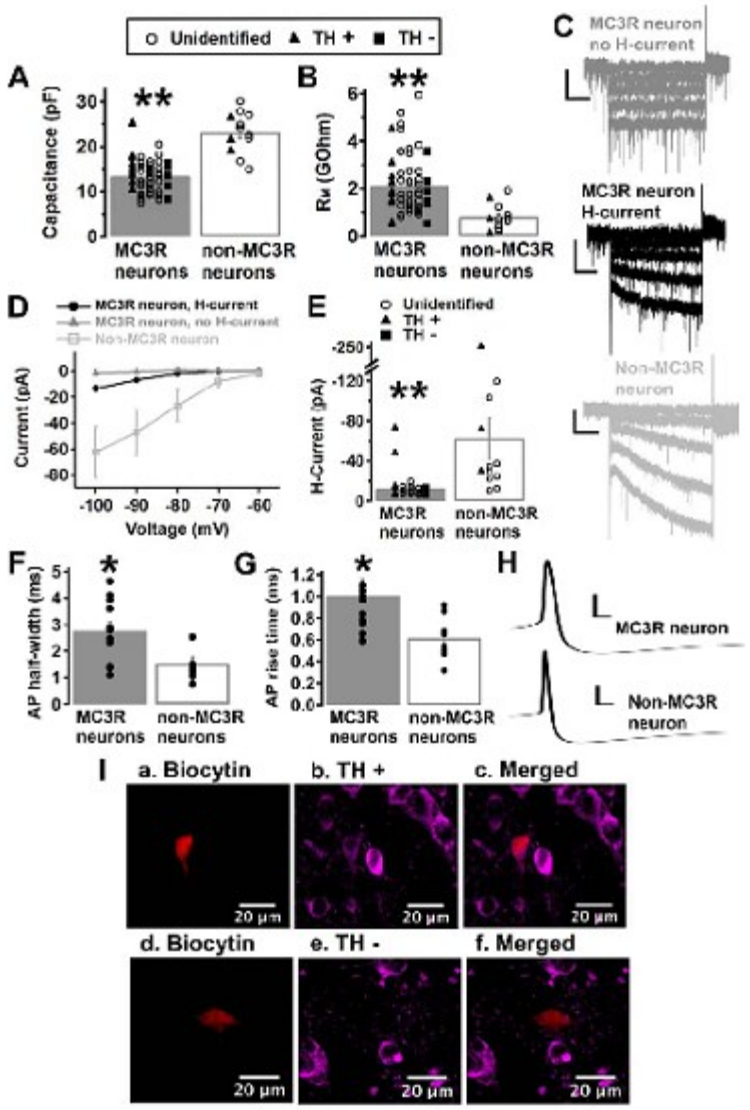

Fig. 3: α-MSH increased the spontaneous firing rate of VTA MC3R neurons in loose cell-attached recordings. A. Sample traces of a MC3R neuron before (black trace) and after (grey trace) α-MSH (1 μM). B. Mean effect of α-MSH on the firing rate of MC3R neurons. C. Mean firing rate of MC3R neurons before and after α-MSH. n= 8 cells from 7 mice. Scale Bars: 1 sec. *p<0.001

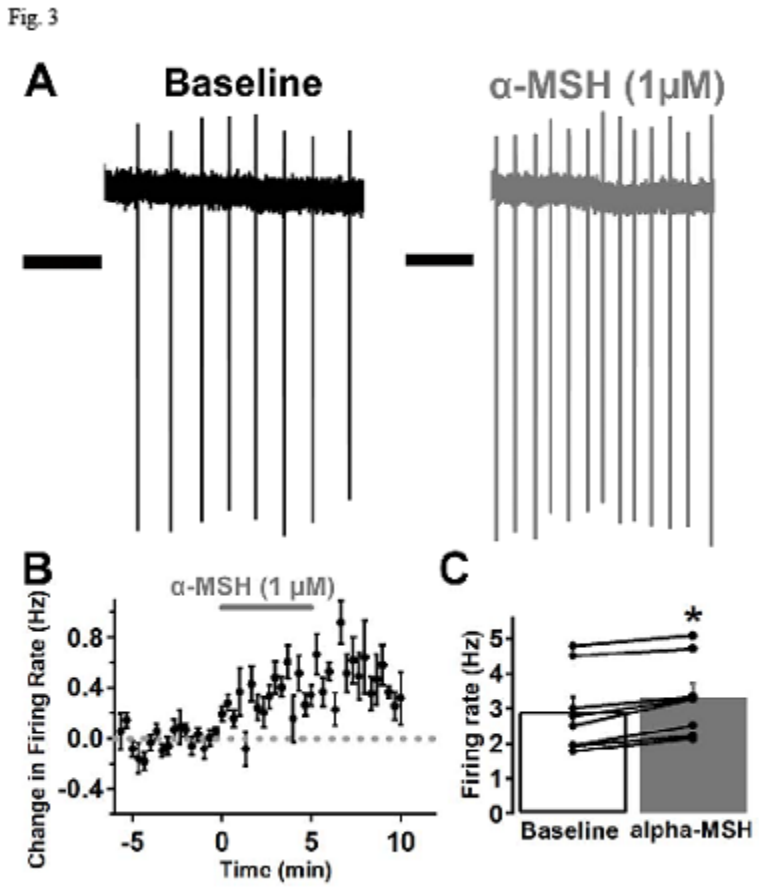

Fig. 4: α-MSH increased the firing rate of VTA MC3R neurons in whole-cell current clamp recordings in the presence of inhibitors of fast synaptic transmission (DNQX: 10 μM; picrotoxin: 100 μM). A. Sample traces of the firing rate of a MC3R neuron before (black trace), during, and after (grey trace) α-MSH (1 μM) application. B,D. Mean effect of α-MSH on the firing rate of MC3R neurons using an internal solution containing 10 mM BAPTA (B) or 1 mM EGTA (D). C,E. Mean firing rate of MC3R neurons before and after α-MSH using an internal solution containing 10 mM BAPTA (C) or 1mM EGTA (E). n= 6 cells from 6 mice for each group. Scale Bars: top trace, 40 mV/1 min; bottom trace, 40 mV/4 sec. *p<0.05

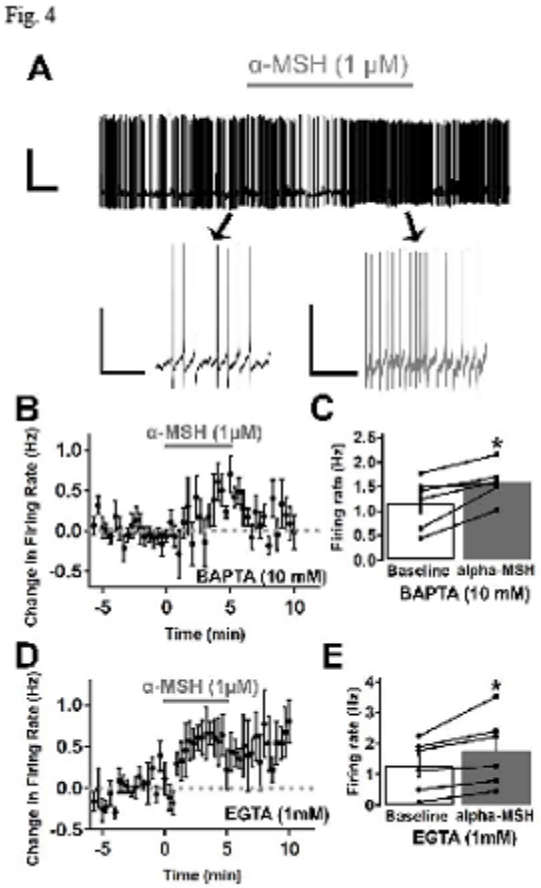

Fig. 5: α-MSH did not increase the firing rate of non-MC3R expressing VTA neurons in whole-cell current clamp recordings in the presence of inhibitors of fast synaptic transmission (DNQX: 10 μM; picrotoxin: 100 μM). A. Sample traces of the firing rate of a non-MC3R neuron before (black trace), during, and after (grey trace) α-MSH (1 μM) application. B. Mean effect of α-MSH on the firing rate of non-MC3R neurons. C. Mean firing rate of non-MC3R neurons before and after α-MSH. n= 5 cells from 5 mice. Scale Bars: top trace, 50 mV/1 min; bottom trace, 40 mV/4 sec.

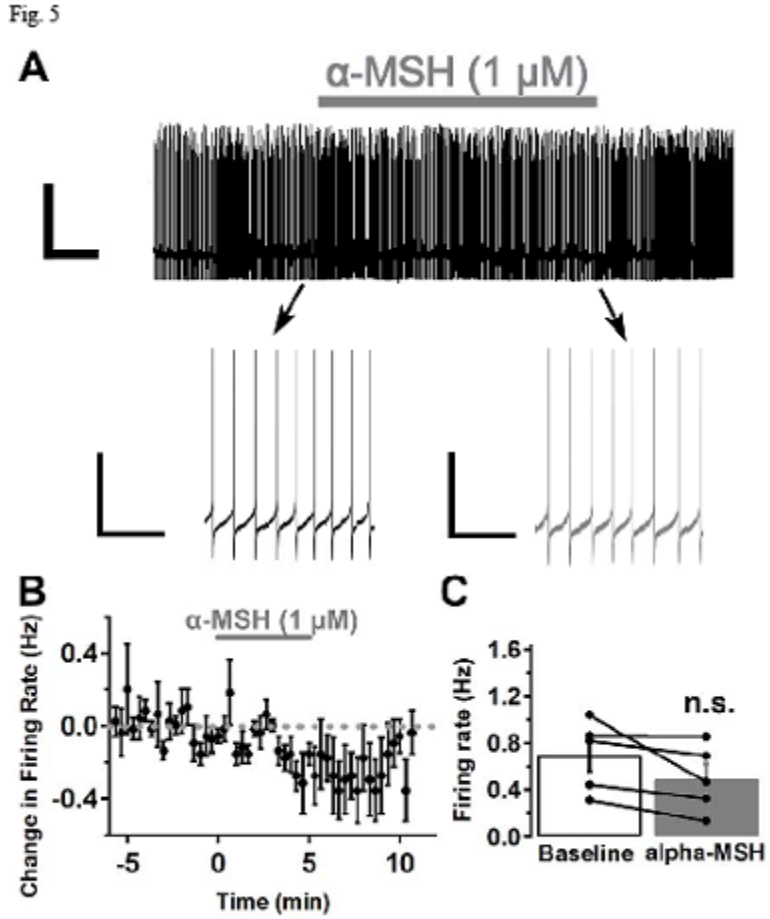

Fig. 6: α-MSH did not significantly affect the membrane potential, current, or resistance of VTA MC3R neurons in the presence of TTX (1 μM). A. Mean effect of α-MSH (1 μM) on the membrane potential of MC3R neurons. B. Mean membrane potential of MC3R neurons before and after α-MSH. C. Mean effect of α-MSH (1 μM) on membrane current of MC3R neurons. D. Mean membrane resistance ($R_M$) of MC3R neurons before and after α-MSH. E. Mean effect of α-MSH on slow voltage ramps (-100 mV to 0 mV 100 mV $s^{-1}$) before (black trace) and after α-MSH (1 μM; grey trace) in MC3R neurons. n= 6 cells from 5 mice for each group.

Fig. 6

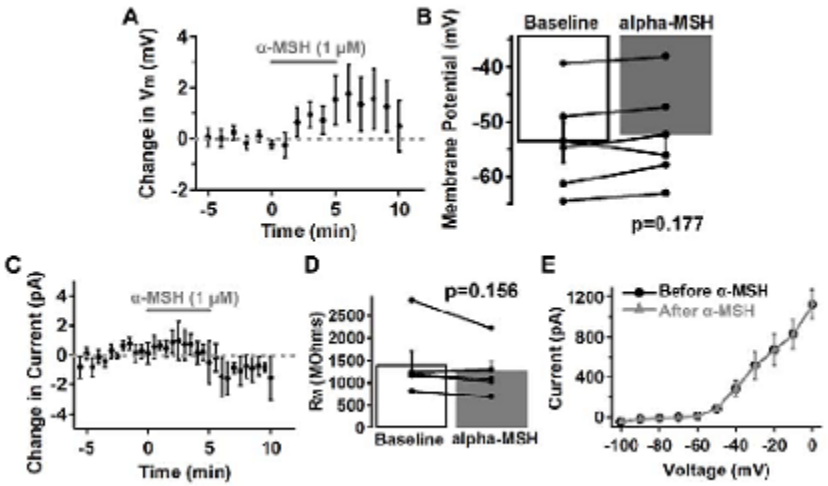

Fig. 7: α-MSH increased the number of current-step evoked action potentials but did not affect rheobase in VTA MC3R neurons. Current steps (2 sec) of increasing amplitude (5-50 pA) were applied every minute before, during, and after α-MSH (1 μM) application. A. Sample traces of a MC3R neuron before (black trace) and after (grey trace) α-MSH. B. Mean effect of α-MSH on the number of action potentials evoked by incrementing 5 pA current-steps (5-50 pA). C-D. Mean effect of α-MSH on membrane potential (C) and mean membrane potential before and after α-MSH (D) for the MC3R neurons in B. E-G. Mean rheobase (the minimum current step required to initiate an action potential; E), mean inter-spike interval at the 40 pA step (F), and mean latency to the first spike at the 40 pA step (G) before and after α-MSH. n= 7-8 cells from 6-7 mice for each group. Scale Bars: left traces, 40 mV/5 sec; right traces, 40 mV/2 sec. *p<0.05

Fig. 7

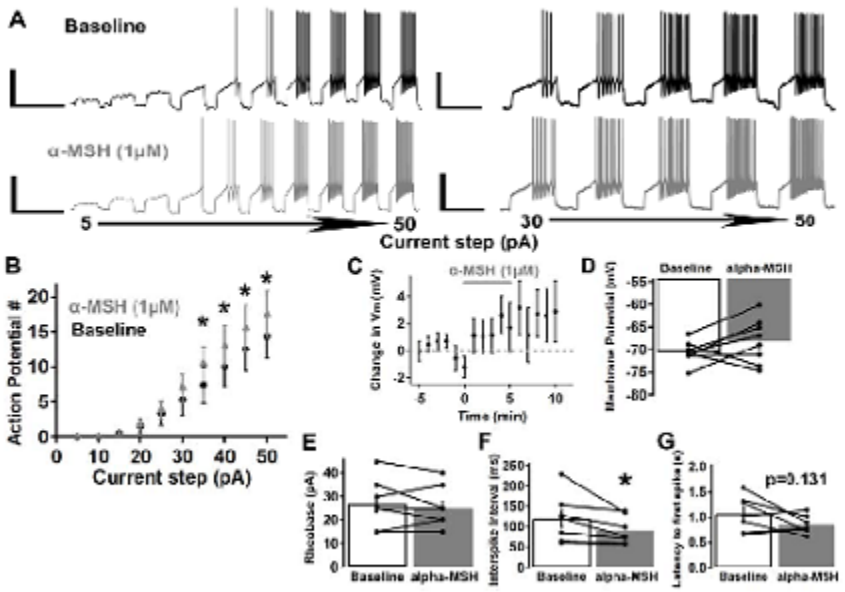

Dr. Katherine West earned her doctorate degree in Neuroscience from Georgia State University (GSU) in 2018. While at GSU, Dr. West worked in Dr. Aaron Roseberry's lab, and studied how the mesocorticolimbic dopamine system regulates feeding, food reward, and body weight and how homeostatic feeding circuits interact with reward circuits. Her dissertation research focused on understanding how hypothalamic neuropeptides, such as α-MSH, alter the activity of ventral tegmental area dopamine neurons. Dr. West also has a bachelor's degree in Biology from GSU. She is currently an Instructor of Biology at Georgia Highlands College.